Universitat de Lleida

Document downloaded from:

The final publication is available at:

Copyright

Disaggregation process for dynamic multidimensional heat flux in building simulation

Roberto Garay Martinez[1]*, Alberto Riverola[2], Daniel Chemisana[2]

[1]Sustainable Construction Division, TECNALIA Research & Innovation, Parque Tecnológico de Bizkaia, C/Geldo s/n, Edificio 700, E-48160 Derio Bizkaia Spain

[2]Sección de Física Aplicada, Universidad de Lleida, Escuela Politécnica Superior, Jaume II, 69, E-25001 Lleida Spain

* Corresponding Author. Tel.: +34 946 430 069, E-mail Address: Roberto.garay@tecnalia.com

Abstract

Heat transfer across envelopes (façade, roof, glazed areas) represents a big share of the energy flow within the heat balance of buildings. This paper focuses on areas of the envelope where multi-dimensional heat transfer occurs. These areas are commonly defined as thermal bridges, due to a localized reduction of thermal resistance of constructions in these places. This paper reviews common standardized methods to assess heat transfer in buildings, under various modelling assumptions: one-dimensional, multi-dimensional, steady state and dynamic. Within presently developed modelling and assessment methods, a need for improvement has been identified over existing methods for the thermal assessment of multi-dimensional heat transfer under dynamic conditions. A phasorial approach to differential heat transfer in thermal bridges has been developed, which serves as the dynamic extension of steady-state thermal bridge coefficients. This formulation is applied to the junction of a masonry wall with a concrete slab.

Nomenclature

Variables

A	Area	m2
C	Response factor (overall heat flow rate)	W/K
c	Response factor (partial heat flow density)	1D: W/m2K
		2D: W/mK
		3D: W/K
d	Thickness of a material layer	M
f	Decrement factor	-
L	Thermal coupling coefficient	3D: W/K
		2D: W/mK
l	Length	m
N	Number of 1D components	-
Q	Heat flow rate	W
q	Density of heat flow rate	W/m2
R	Thermal resistance	m2K/W
T	Temperature	K
U	Surface thermal transmittance, Thermal transmittance	W/m2K
Y	Periodic thermal transmittance	W/m2K
λ	Thermal conductivity	W/mK
θ	Phase of vector	-
φ	Phase difference	hour
χ	Point thermal transmittance	W/K
Ψ	Linear thermal transmittance	W/mK

Subscripts

BC	Boundary condition
e	External
ei	Exterior-interior
i	Internal
ii	Interior-interior
se	External surface
si	Internal surface
t	Time
tot	Total
$1D$	1-dimensional
$2D$	2-dimensional
$3D$	3-dimensional
$1,2,3,...n$	Individual layers in a 1D construction
i, j, k	Individual elements
y	Individual time step
^	Harmonic property
.	Instantaneous value

1. Introduction

Up to 40% of primary energy consumption in developed countries is related to buildings [1] [2] [3] [4], where a large share is used for space heating and cooling, to meet occupants' comfort requirements. The scientific community has conducted Intensive studies and developed techniques for the assessment of heating, cooling and air conditioning energy consumption of buildings over more than 50 years. At present times, various test and calculation methods are

available, which focus on different scales and approaches for the assessment of thermal performance of buildings, from standardized material testing procedures to dynamic simulation software tools [5].

Heat transfer across building envelopes has a significant influence on the heat balance of buildings. Building envelopes are the physical interface between indoor and outdoor conditions, and their response to variations on these conditions, such as temperature oscillations and incidence of solar radiation, substantially defines the heat dynamics of buildings. For this reason, building codes impose many requirements on the steady state performance metrics of envelopes, such as maximum allowances on the thermal transmittance of envelopes, window ratio, overall heat loss coefficient, etc.

The dynamic performance of buildings is commonly assessed by means of simulation. In this field, Building Energy Simulation (BES) tools have been developed over the last decades with increasing accuracy. Software tools such as EnergyPlus [6] and TRNSYS [7] have evolved to such a level of complexity that their accuracy is commonly related to modelling assumptions and input data introduced by users of these tools, rather than by the tools themselves. Strachan et al. [8] performed a comparative analysis of simulation outputs from several researchers on very detailed validation experimental campaigns.

However, some fields still remain where building simulation tools have not been fully developed or their use has not been fully introduced to the building simulation community. Simulation tools are in constant evolution to meet simulation needs imposed by new construction techniques, dynamic systems and highly insulated houses such as Nearly Zero Energy Buildings (NZEB).

NZEBs are characterized by a substantial improvement in envelope insulation levels compared with state of the art construction methods, along with reductions on heat losses related to ventilation & air infilatration and the introduction of renewable energy systems. Within such environments, thermal bridges are no longer a minimal part of the heat balance of a building, but may play a significant role in it. In [9] a numerical and experimental study was carried out over a well-insulated steel-frame lightweight construction, similar to many commercially available insulation systems. In this work, thermal bridges were found to cause an increase of 13-27% in the one-dimensional heat transfer coefficient of a wall.

In practical applications for the calculation of heating & cooling loads in buildings, thermal bridges are usually considered by means of simplified approaches. In ASIEPI [10] a detailed review of simulation software was performed and atlases [11, 12, 13] were published for building physicists. Thermal bridge atlases and best practice/accredited construction details are available in [14, 15, 16]. A review on normative compliance regarding thermal bridges in European countries [17] highlighted differing compliance and assessment methods, where various parameters were assessed, such as temperature factor, lineal thermal transmittance, etc. Overall, while assessment methods for each country may differ, most of them are based on the application of thermal bridge atlases and default values.

Several previous works such as [18] have identified that the thermal insulation level of building envelopes can be improved up to 18% with a correct design of junctions between adjacent envelope constructions. In [19] several building envelope studies were reviewed, summarizing that the multi-dimensional thermal performance of a wall reaches a 27%-80% deviation from one-dimensional heat transfer analysis. In [20], the thermal bridge of several architectural junction details is assessed, where thermal bridge coefficient values according to [21] are

positioned in the range of 0.59-1.02 W/mK for floor-wall junctions in several masonry wall configurations.

The evolution of various cases of thermal bridges before and after envelope insulation works is evaluated in [22, 23].

In order to bring the aforementioned figures from [21] to the context of highly insulated envelopes, the lower figure (0.59 W/mK) is akin to the heat loss coefficient of a wall with a U-value of 0.2 W/m2K within a 3m slab-to-slab height configuration (0.6 W/mK).

For assessing multi-dimensional heat transfer, different reference dimensions can be taken. Methodological inconsistencies due to this and other factors are discussed in [23]. In [24], discrepancies in results attributed to different geometrical definitions of the dimensions of thermal bridges are presented.

Considering that the relevance of multi-dimensional heat transfer in building envelopes is increasingly impacting the heat balance of buildings in the path to NZEBs, new methods need to be developed for the proper computation and assessment of these areas. In this field, previous works have dealt with calibration and identification techniques of dynamic models for thermal bridges.

Up to very recently the evolution of computational techniques for the assessment of energy consumption in buildings paid only marginal attention to multi-dimensional heat transfer. In the development of building simulation codes, predominant energy paths (homogeneous walls, fenestration…) were prioritized, furthermore considering the comparably higher computational effort required to properly address multi-dimensional heat transfer.

Numerical modelling for multi-dimensional heat transfer is most commonly not covered by building simulation codes and performed under normalized steady-state boundary conditions [21]. Outcomes from these calculations can be introduced into building simulation codes by means of steady-state thermal performance parameters. To the authors' belief, these simplified procedures should be amended. In this belief, it is considered that within highly insulated buildings, the deviation of simplified steady-state assessments from a proper dynamic thermal modelling of thermal bridges is increased.

Dynamic numerical models for architectural junctions have been developed in [25, 26, 27, 28], where discretization methods such as finite element and finite difference methods are used. In [29], linear thermal bridges were modelled using a Boundary Element Model in the frequency domain. In [30, 31], a procedure for obtaining the z-transfer function of 3-dimensional thermal bridges is developed. In [28], dynamic heat flows for timber frame constructions are provided in terms of amplitude and phase shift parameters, under various modelling approaches. In this same work, it is concluded that additional information is required for incorporating dynamic models into BES software in order to properly model thermal bridge elements. This approach is preferred due to its accuracy when compared to the introduction of equivalent parameters into a one-dimensional heat transfer model for homogeneous walls. In equivalent-wall methods defined in [26], the architectural detail of the junction is reduced to minimize the overlapping between the dynamics of the thermal bridge and the dynamics of the homogenous wall portions, when compared to standardized geometric requirements in [21]. Therefore, it could be concluded that the dynamics of a thermal bridge differ from the dynamics of homogeneous walls, and that a specific disaggregation procedure for their dynamic modelling would be desirable.

To the authors' belief, considering different dynamic performance of homogeneous walls and architectural junctions identified in [26] and the recommendation for developing specific models for architectural junctions in [28], a generalized geometrical and calculation procedure is needed to properly assess dynamic heat transfer in architectural envelopes. In order to integrate this procedure into the wide range of formulae used by researchers and engineers in the field of building physics, this calculation procedure should be based in commonly used and standardized definitions and calculation procedures [21, 32, 33, 34, 35]. In this generalized methodology, full compatibility of the formulae with geometrical dimensions in [21] and variables defining steady-state and dynamic performance in [34, 32] should be pursued.

Generalized formulae following this approach would avoid uncertainties in the calculation of dynamic thermal properties by methods such as [26], where the dynamically affected envelope area needs to be defined by calculation and inspection for each particular case, and thus the obtained heat transfer function is only applicable to that particular case. Furthermore, with the methodology in [26], the geometrical definition of building envelopes needs to be modified for each architectural junction within a building simulation model, requiring extensive effort in the process. Generalized formulae aligned with the geometrical definitions in [21] would substantially facilitate transitions between thermal assessment works at architectural junction level and full-scale building energy simulation.

In this paper, a mathematical formulation is developed, following the generalization criteria defined above, for the disaggregation of dynamic heat transfer phenomena in envelope areas with multi-dimensional heat transfer. This formulation provides the opportunity to differentiate the dynamic thermal performance of a thermal bridge from dynamic one-dimensional heat transfer in detailed numerical calculations – e.g. performed by means of finite element models. The proposed approach provides output which can later be introduced in BES tools for a coupled analysis within a full-building simulation.

2. Dynamic models for building envelopes

Building envelopes represent a relevant share of the heat exchange between the building and its environment. Envelopes are the physical boundary of buildings and are designed to shelter occupants from variable outdoor conditions. Due to the variability of these conditions, heat transfer across the envelopes is highly dynamic.

Regarding the energy behaviour of building envelopes, three main categories are identified:

- Fenestration systems, curtain wall elements, etc. These systems show a high permeability to solar radiation, along with a reduced thermal mass. For their characterization, two steady-state equations are used, describing short-wave energy input from the sun and thermal heat transfer with the environment (long wave radiative, convective, and conductive heat transfer). [36, 37]
- Lightweight insulated envelope systems, sandwich panels, etc. These systems are distinguished by a minimal thermal mass and relatively high thermal resistance. In such envelopes, thermal inertia is of little relevance, and useful thermal models can be obtained by means of one steady-state equation.
- Massive envelope systems, stonework, masonry, brickwork, etc. Thermal inertia in these constructions allows for a substantial smoothing and phase shifting of thermal effects caused by oscillating boundary conditions. In order to achieve a suitable characterization of these systems, several mathematical formulations can be used.

Some of the most commonly used models are based on transfer functions and response factors.

In this paper, thermal performance calculations for massive construction elements are addressed. As stated above, the inertia of these systems provides a relevant smoothening of the response of walls to varying boundary conditions. For comparative calculations, wall performance is commonly assessed by means of the steady-state thermal transmittance value of a wall. This parameter provides the benefit of allowing its comparison with fenestration systems.

Although steady-state thermal transmittance is considered to be a good performance indicator for fenestration and lightweight insulated systems, the assessment of the thermal performance of massive walls requires further characterization of the dynamics of the wall.

For the dynamic thermal performance modelling of building envelopes, techniques such as discrete transfer functions, response factors, finite elements, finite differences and phasor approaches are used. Each of the mentioned alternatives is used in different contexts given its particular ratio between accuracy and computational cost.

BES software tools such as EnergyPlus [6] and TRNSYS [7] perform (multi) yearly simulation of the energy performance of whole buildings, where the thermal response of walls and other thermal systems is computed at regular hourly or sub-hourly intervals. In this context, the computational effort required for the computation of each wall assembly is critical. EnergyPlus bases its calculations in the so-called "Conduction Transfer Function", while TRNSYS uses the Mitalas Transfer Function. In both cases, these functions model the heat transfer across a wall based on present and past values of surface temperature and heat flux of the wall.

One-dimensional models based on multi-element/difference discretization of a wall require much larger computational effort and are commonly disregarded for standardized calculations in BES systems, although these are implemented in optional algorithms [6].

For the dynamic performance assessment of building envelopes, EN 13786 [32] provides a calculation method in which the one-dimensional dynamic thermal performance of a wall under harmonic boundary conditions can be obtained.

In this work, a multi-dimensional generalization of [32] is provided, in which boundary conditions are defined similarly, but its heat transfer calculation method is substituted by a numerical method –i.e. finite element method. The selected numerical method provides an accurate modelling of the multi-dimensional heat transfer under similar geometrical modelling conditions as defined in [21], and an accurate modelling under dynamic conditions as to obtain the time-variant thermal response of the system through the output parameters in [32].

Under this approach, a dynamic generalization of parameters in [21] is achieved, compatible with the parameter definition in [32].

3. Relevant standardized procedures for thermal assessment

The proposed dynamic thermal assessment builds over several international standards, and generalizes the dynamic thermal assessment of multi-dimensional heat transfer by means of the hybridization of two standards [21, 32]. The relevant international standards for the topic of this paper are reviewed below.

In ISO 7345 [33], physical quantities and corresponding symbols and units used in the thermal insulation field are defined.

The method to obtain the thermal resistance and thermal transmittance of building components and elements is provided in EN 6946 [34]. It is important to note that this procedure excludes doors, glazed units, curtain walling, components which involve heat transfer to the ground, and components allowing air permeability. The method assesses the appropriate design thermal conductivity or thermal resistance of the materials considering their application. This calculation procedure applies to thermally homogeneous layers, including air layers and cavities. Relevant parameters defined [34] are thermal resistance (R) and thermal transmittance (U). The thermal resistance of a homogeneous material is defined in (1), the total thermal resistance of a building component is calculated in (2), and the thermal transmittance is obtained in (3).

$$R = \frac{d}{\lambda} (X) \tag{1}$$
$$R_T = R_{si} + R_1 + R_2 \ldots + R_n + R_{se} \tag{2}$$
$$U = \frac{1}{R_T} \tag{3}$$

Numerical calculation of heat flows and minimum surface temperatures in steady-state multi-dimensional heat transfer environments are defined in EN 10211 [21]. The specification for two-dimensional and three-dimensional geometrical models of thermal bridges is performed in this standard. Geometrical boundaries, model subdivisions, thermal boundary conditions and thermal values and relationships are incorporated within the specifications. In addition, the procedure for obtaining linear and point thermal transmittances and surface temperature factors is explained.

The thermal coupling coefficient L_{3D} between two different environments can be obtained from the total heat flow Q calculated three-dimensionally in (4).

The thermal coupling coefficient obtained from 2D calculation L_{2D} of the component separating two different environments can by derived from the heat flow, as defined in (5).

$$Q = L_{3D}(\theta_i - \theta_e) \tag{4}$$
$$Ql = L_{2D}(\theta_i - \theta_e) \tag{5}$$

Based on the definitions given in (3, 4 and 5), the linear thermal transmittance (Ψ) separating two environments is defined in (6), and the point thermal transmittance (χ) is defined in (7).

$$\Psi l = L_{2D} - \sum_{j=1}^{N_j} U_i A_i \tag{6}$$

$$\chi = L_{3D} - \sum_{i=1}^{N_j} U_i A_i - \sum_{j=1}^{N_j} \Psi_j l_j \tag{7}$$

EN 13786 [32] provides methods to calculate the harmonic thermal behavior of a complete building component where one-dimensional heat transfer can be assumed. In this document,

the periodic thermal transmittance (Y_{mn}) and the decrement factor (f) are defined. In this method, the response of a wall to harmonic excitations is assessed.

The periodic thermal transmittance is defined as the complex amplitude of the density of heat flow rate through the surface ($\hat{q}_i$), divided by the complex amplitude of the harmonic temperature excitation ($\widehat{T}_e$). Magnitudes on opposite sides of the wall (m and n) are taken to define the transmittance.

The decrement factor (f) is defined as the ratio of the modulus of the periodic thermal transmittance to the steady-state thermal transmittance U.

$$Y_{e,i} = -\frac{\hat{q}_i}{\widehat{T}_e} \tag{9}$$

$$f = \frac{|\hat{q}_i|}{|T_e|U} = \frac{|Y_{e,i}|}{U} \tag{10}$$

The phase difference (φ) measures the difference in hours between the peak excitation (maximum exterior temperature) and its response (peak heat density of heat flow rate at the interior surface).

When considering a phasorial approach to the phase difference defined in [32], this phase difference needs to be converted into an angular shift. In this operation, the magnitude of the phase difference is related to the period of the considered periodic boundary condition, as per equation (11).

$$\theta = \frac{\varphi}{Period} * 2\pi \tag{11}$$

4. Phasorial approach to dynamic thermal properties

According to [38], *"…a phasor… is a complex number representing a sinusoidal function whose amplitude (A), angular frequency (ω), and initial phase (ϑ) are time-invariant. …. The complex constant, which encapsulates amplitude and phase dependence, is known as phasor..."*

With a fully developed algebraic operation system, phasor operations can be used to perform addition or subtraction operations in dynamic linear systems such as building envelope systems, under uniform frequency conditions. Within a heat transfer equation, different phasors can be used to represent different heat flows in an architectural detail with multi-dimensional heat flow. This can be represented as shown in eq. (12.a, 12.b), which can be further transformed to meet the definitions in section 8.2 of [21], as shown in eq. (13.a, 13.b)

Equations (12.a, 13.a) show steady-state base formulation in [21] while in (12.b, 13.b) its phasorial variant is formulated. Furthermore, given the definition of Y in [32], eq. (13.b) is further converted in eq. (14) to compatibilize it with [32].

$$Q_{tot} = \sum_{1D} Q_i + \sum_{2D} Q_j + \sum_{3D} Q_k \tag{12.a}$$

$$Q_{tot}\angle\theta_{tot} = \sum_{1D} Q_i\angle\theta_i + \sum_{2D} Q_j\angle\theta_j + \sum_{3D} Q_k\angle\theta_k \tag{12.b}$$

$$L_{3D}\angle\theta_{tot} = \sum_{1D}(U_i * A_i) + \sum_{2D}(\psi_j * l_j) + \sum_{3D}(\chi_k) \tag{13.a}$$

$$L_{3D}\angle\theta_{tot} = \sum_{1D}(U_i\angle\theta_i * A_i) + \sum_{2D}(\psi_j\angle\theta_j * l_j) + \sum_{3D}(\chi_k\angle\theta_k) \tag{13.b}$$

$$L_{3D} \angle \theta_{tot} = \sum_{1D}(Y_i \angle \theta_i * A_i) + \sum_{2D}(\psi_j \angle \theta_j * l_j) + \sum_{3D}(\chi_k \angle \theta_k) \qquad (14)$$

The transition of eq. (12.b) and (13.b) is performed as a phasorial implementation of (4, 5), where given only one periodical boundary condition in a thermal model, $L_{tot} \angle \theta_{tot}$ can be calculated according to eq. (15):

$$Q \angle \theta = L_{tot} \angle \theta_{tot} * T_{BC} \angle 0 \qquad (15)$$

For situations with multiple boundary conditions with the same oscillation periods in an architectural detail, $Q_{tot} \angle \theta_{tot}$ can be obtained with the phasor-equivalent method to the one stated in section 8.3 of (11), as shown in eq. (16).

$$Q_{tot} \angle \theta_{tot} = \sum_{BC}(L_{tot,BC\_n} \angle \theta_{tot,BC\_n} * T_{BC\_n} \angle \theta_{BC\_n}) \qquad (16)$$

5. Calculation procedure of the phasorial assessment of differential heat transfer in thermal bridges

The application of phasor operators to the dynamic heat transfer analysis of a thermal bridge is reflected by means of eq. (14, 16). However these equations contain many heat transfer coefficients which need to be obtained in a hierarchized way. In this section, a stepwise approach for obtaining phasorial coefficients for an architectural junction is defined. This approach is applied to a case study in section 6.

Similarly to steady-state calculations under [21], the initial step is the construction of a multidimensional geometrical model, comprising all the architectural junctions to be assessed in the analysis. The main particularity in the scope of this model is its purpose to assess dynamic heat transfer; for this purpose, thermal conductivity/resistance of materials is complemented by material density and specific heat. The amplitude and phase shift of the heat flux on the inner surfaces of the model are obtained.

Additional models are constructed to obtain the heat flux across partial subsets of the architectural junction (e.g. 1D heat transfer for 2D architectural detail). Again, amplitude and phase shift of the heat flux are taken on the inner surface of the model.

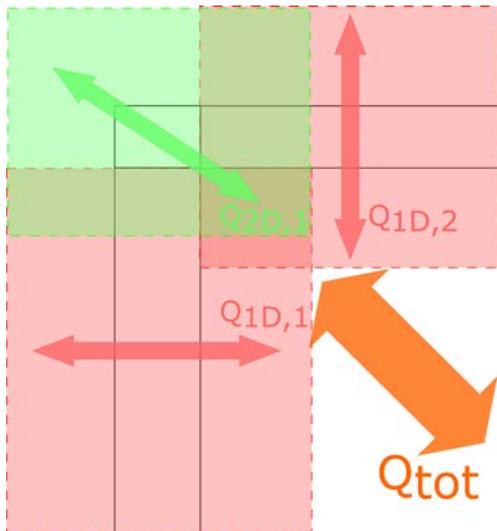In figure 1, heat paths in a 2D architectural detail are shown, along with their phasor representation.

Figure 1: Sketch of an architectural junction with a geometrical thermal bridge (left), and its phasor representation (right).

In table 1, the calculation steps to obtain the required parameters in eq. (14) are provided. For 2D architectural models, only steps 1-3 will be required.

Table 1. Calculation steps to achieve all the required heat transfer data in eq. (14)

Step	2D	3D	Action	Obtained data
1	Yes	Yes	Construct 1D heat transfer models	$L_{1D}\angle\theta_{tot}$
2	Yes	Yes	Eq. (14) without 2D and 3D heat transfer	1D, all Y and θ parameters
3	Yes	Yes	Construct 2D heat transfer models	$L_{2D}\angle\theta_{tot}$
4	Yes	Yes	Eq. (14) without 3D heat transfer	2D, all ψ and θ parameters
5	n/a	Yes	Construct 3D heat transfer models	$L_{3D}\angle\theta_{tot}$
6	n/a	Yes	Eq. (14)	3D, all χ and θ parameters

This sequence needs to be followed for each particular oscillation frequency/period in the boundary conditions.

A graphical representation of the calculation procedure is provided in Figure 2. This sequence needs to be performed for each particular oscillation frequency study.
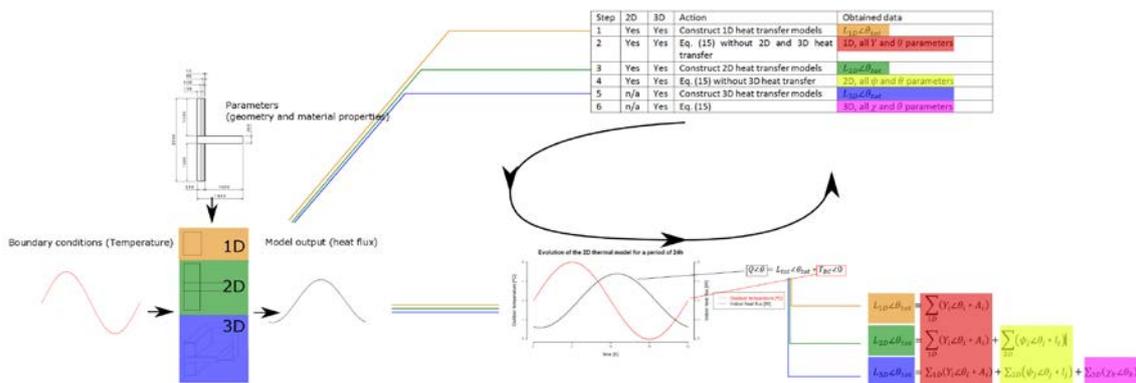
Figure 2. Calculation sequence and solving of equations (15) and (16) according to steps defined in Table 1.

In some particular cases, where the architectural model has been constructed in such a way where its edges are not affected by the junction, the heat flux of partial subsets can be obtained from the main model, by obtaining heat transfer data from cut planes at the edge of the model. However, this approach needs to be validated for each particular case and applied with caution.

6. Case study

In order to identify the relevance of dynamic phenomena in thermal bridges, and the outcomes of the defined methodology, a case study has been defined and solved. A junction of an external wall with an intermediate floor slab has been selected for this purpose. This junction is typical of masonry constructions in Spain and other South European countries, where thermal mass can have a relevant influence in the avoidance of overheating in summer periods.

A single-leaf ceramic masonry construction with internal insulation and internal plasterboard lining has been selected for the building envelope. This type of wall assembly is representative of typical construction details built in Spain after the 2006 Construction Building Code.

Following common construction details in Spain, this masonry construction is supported on the edges of a floor slab with structural properties. Considering this, the intersection is constructed in such a way that the slab is exposed to the external ambience. These construction details are well known causes of poor thermal performance of building envelopes.

This case study is a simple yet common construction detail in South European countries. To the authors' opinion, it is best suited to illustrate the proposed methodology. The construction of the junction is relatively simple, avoiding unnecessary complexities in the description within the manuscript. Furthermore, due to the two-dimensional nature of this junction, the reader is provided of graphs and figures with more precise details compared to potential three-dimensional alternatives.

6.1 Geometry

The modelled façade-slab junction is defined by the dimensions and compositions indicated in Table 2.

Table 2: Composition of the model

Element	Thickness [mm]	Modelled distance from junction [mm]	Composition
Façade, above slab	310	1500	According to Table 3
Façade, below slab	310	1500	
Floor slab	300	1810	Concrete

The model height is set to 3.3 meters, where 3 meters correspond to the internal height of the external wall between slabs and 0.3 meters correspond to the height of the slab. All calculations refer to the 3.3 m model height (external dimensions of the façade). The wall thickness is 0.310 meters and there is a distance of 1.5 meters from the internal surface to the cut plane of the slab. This geometry is depicted in Figure 3.

For the calculation of linear thermal coefficients, this geometry results in an external height of 3.3m and an internal height of 3m for the considered model.
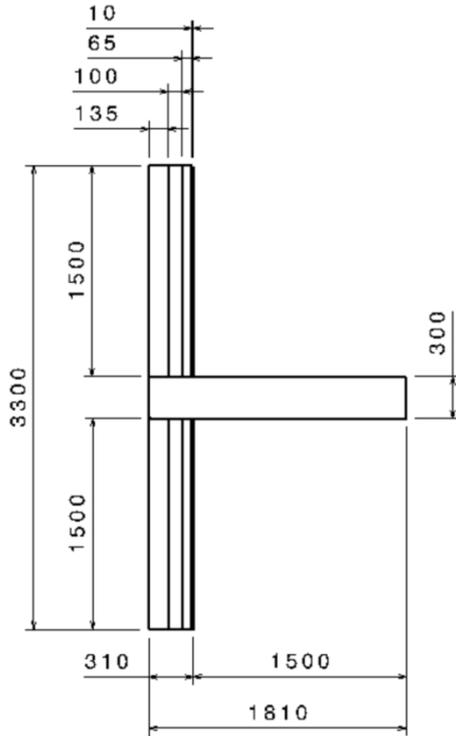

Figure 3: Model dimensions (in mm)

The composition and thermal properties of each assembly are shown in Tables 3 (masonry wall) and 4 (concrete slab).

Table 3: Thermal properties of the wall

Position	Element	Thickness [m]	Thermal Resistance [m²K/W]	Thermal Conductivity [W/mK]	Density [kg/m³]	Specific Heat [J/kgK]
Exterior	Brick	0.135	0.193	0.700	1600	850.0
	Extruded polystyrene	0.100	2.857	0.035	25	1470.0
	Air gap*	0.065	0.180	0.560	1.185	1004.4
Interior	Plasterboard	0.010	0.020	0.500	1300	840.0

Material data are taken from [28], while the thermal resistance of the air gap is taken from [39] for the case of horizontal heat flux.

Table 4: Thermal properties of the concrete slab

Element	Thickness [m]	Thermal Conductivity [W/mK]	Density [kg/m^3]	Specific Heat [J/kgK]
Concrete	0.300	2.600	2300	930

6.2 Numerical model

The numerical assessment of this construction junction has been performed using a multi-dimensional finite difference method. Commercial software developed by PHYSIBEL [40] has been used. Within the same software suite, programs VOLTRA [41] (dynamic) and TRISCO [42] (steady-state) have been used to perform the required calculations.

Additionally to the dynamic study assessing dynamic thermal performance according to the mathematical formulation in (14), a steady-state thermal model was performed. In Table 5, the imposed boundary conditions for steady-state and dynamic analysis can be observed. In Figure 4, boundary conditions are depicted over the modeled geometry. Detailed dimensions and composition of each layer can be found in figure 4.
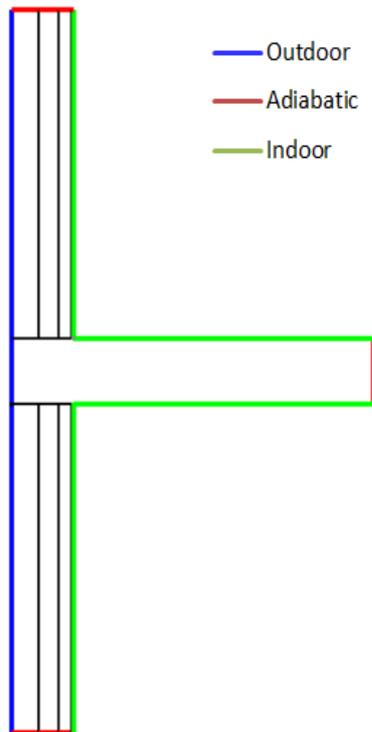

Figure 4: Geometrical definition of boundary conditions

Table 5: Boundary conditions

Assessment	Position	Heat transfer	Mean	Temperature	Period

type		Coefficient [W/m^{2}K]	temperature [°C]	amplitude [°C]	[h]
Steady-state	Outdoor	25	0	-	-
	Indoor	7.69	20	-	-
Dynamic	Outdoor	25	0	10	Variating, refer to Table 6
	Indoor	7.69	0	0	-

6.3 Steady-state performance

The case study resulted in an equivalent thermal transmittance of 0.696 W/m^{2}K. Considering that the one-dimensional thermal transmittance of the façade is 0.298 W/m^{2}K, the thermal bridge coefficient of the façade-slab junction, Ψ is calculated at 1.312 W/mK. In Figure 5, a vertical section of the temperature field is shown.
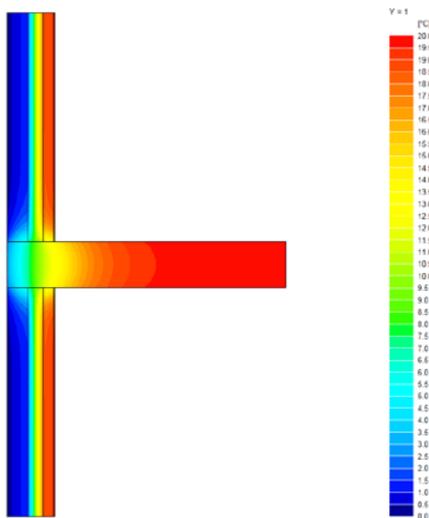

Figure 5: Temperature distribution [ºC]

Under the aforementioned steady-state approach, the 2-dimensional case shows a 134% increase in heat flow due to the wall-slab junction when compared to one-dimensional analysis of the external wall

For the modelled case, with a 3 m slab-to-slab height, this implies that the thermal bridge represents 57% of the total heat transfer across the external wall. Considering that the model height is representative of the building stock, the reduction in the insulation level observed in this steady-state analysis can be transposed to an equivalent increase in the thermal coupling coefficient of the whole wall.

6.4 Dynamic performance

The dynamic thermal performance was assessed for various oscillation periods of the external boundary temperature. For every case, evolutions of heat flow density and temperature were obtained. Simulation time was defined such as to allow for the stabilization of heat flow oscillations. In all cases, more than 10 periods were simulated to ensure the proper thermal initialization of the construction junction.

Oscillation periods in the range of 1 to 1728h were computed, with various intermediate resolutions. Simulation periods were spaced by 1h for periods shorter than 36h. For longer periods, the spacing was increased to 3h until 60h, 6h until 84h, 12h until 120h and 24h until 1728h. In Table 6, an excerpt of the results can be seen.

For each case, periodic thermal transmittance, decrement factor and phase difference (φ) were obtained according to ISO 13786. Output variables of the proposed methodology according to the process defined in Table 1 were calculated. All this information is presented in Table 6. In Figure 6, the evolution of temperature and heat flux is shown for the dynamic simulation of the system for a period of 24 hours.
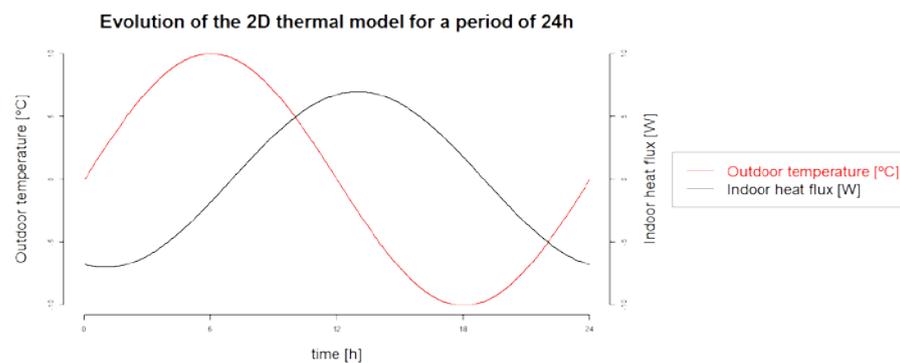

Figure 6: Dynamics of temperature and heat flow in the dynamic assessment of the external wall-intermediate slab junction for the period of 24h

Table 6: Dynamic properties

Time [h]	Amp q_{1D} [W]	Amp q_{2D} [W]	Time shift φ_{1D} [s]	Time shift φ_{2D} [s]	Y_{1D} [$\frac{W}{m^2K}$]	Y_{2D} [$\frac{W}{m^2K}$]	ΔY [$\frac{W}{m^2K}$]	Phase θ_{1D} [rad]	Phase θ_{2D} [rad]	Ang ΔY [rad]
3	0.08	0.08	9143	9150	0.008	0.008	0.000	1.69	1.69	-0.28
6	0.35	0.37	12180	12540	0.035	0.037	0.004	1.13	1.16	1.48
9	0.63	0.69	14400	15210	0.063	0.069	0.012	0.89	0.94	1.24
12	0.88	1.00	16200	17520	0.088	0.100	0.021	0.75	0.81	1.10
18	1.31	1.58	19080	21600	0.131	0.158	0.045	0.59	0.67	0.92
24	1.65	2.12	21120	25200	0.165	0.212	0.072	0.49	0.58	0.82
32	1.99	2.75	22800	29100	0.199	0.275	0.110	0.40	0.51	0.71
42	2.28	3.42	24300	33000	0.228	0.342	0.152	0.32	0.44	0.61
48	2.40	3.76	24900	34800	0.240	0.376	0.173	0.29	0.40	0.57
54	2.50	4.06	25500	36600	0.250	0.406	0.194	0.26	0.38	0.53
60	2.57	4.34	25800	38100	0.257	0.434	0.213	0.24	0.35	0.49
72	2.68	4.79	26400	40500	0.268	0.479	0.244	0.20	0.31	0.43
84	2.75	5.16	26700	42300	0.275	0.516	0.270	0.18	0.28	0.38
96	2.80	5.45	26850	43800	0.280	0.545	0.291	0.16	0.25	0.35
120	2.86	5.86	27150	45900	0.286	0.586	0.320	0.13	0.21	0.29
144	2.90	6.14	27300	47325	0.290	0.614	0.340	0.11	0.18	0.25
192	2.93	6.45	27450	48600	0.293	0.645	0.362	0.08	0.14	0.19
240	2.95	6.62	27450	49500	0.295	0.662	0.374	0.06	0.11	0.15
288	2.96	6.72	27450	49800	0.296	0.672	0.381	0.05	0.10	0.13
336	2.96	6.78	27600	50100	0.296	0.678	0.385	0.05	0.08	0.11
384	2.97	6.82	27600	50400	0.297	0.682	0.388	0.04	0.07	0.10
432	2.97	6.85	27600	50550	0.297	0.685	0.390	0.04	0.07	0.09
480	2.97	6.87	27600	50550	0.297	0.687	0.391	0.03	0.06	0.08

In Figure 7, one-dimensional and two-dimensional periodic thermal transmittance values are presented, along with the differential thermal transmittance associated with the thermal bridge. For short oscillation periods, the thermal mass in the construction isolates the indoor environment from oscillations in the outdoor environment, leading to negligible Y values. Also, due to the fast oscillations, the time shift exceeds the period of the oscillations, leading to phase shifts greater than 2*pi.

For longer oscillation periods, greater Y values are obtained, leading to pseudo-stationary behavior when the oscillation period substantially excedes the time constant of the system. In these cases, the phase shift is practically non-existent.
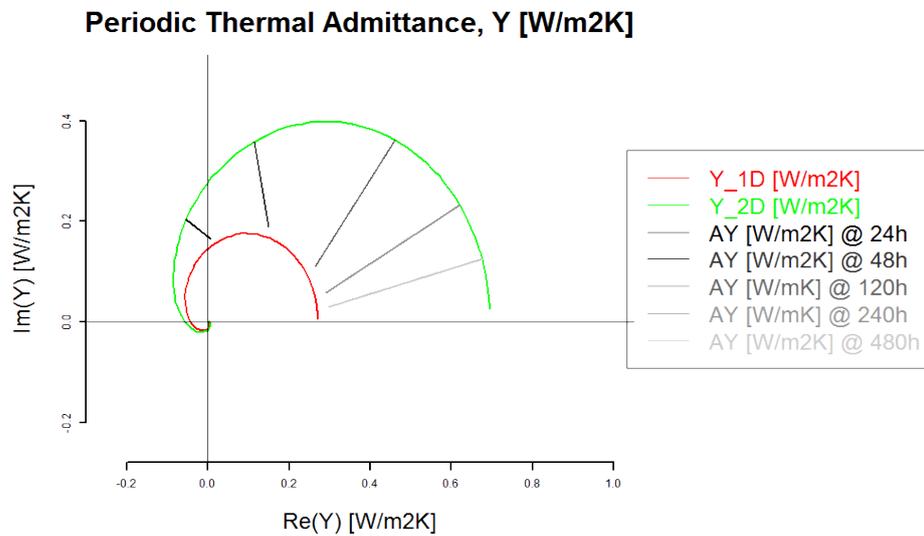
Figure 7: Phasor representation of the thermal response of the architectural junction

In Figure 8, the delay in the response is shown, in both phase and time shift. Maximum phase shift is observed for short oscillation periods. However, the maximum shift in time is observed for long oscillation periods. Maximum time shifts are observed for oscillation periods at 100h (1D) and 200h (2D), where time shifts of 7.7h (1D) and 14.25h (2D) happen.
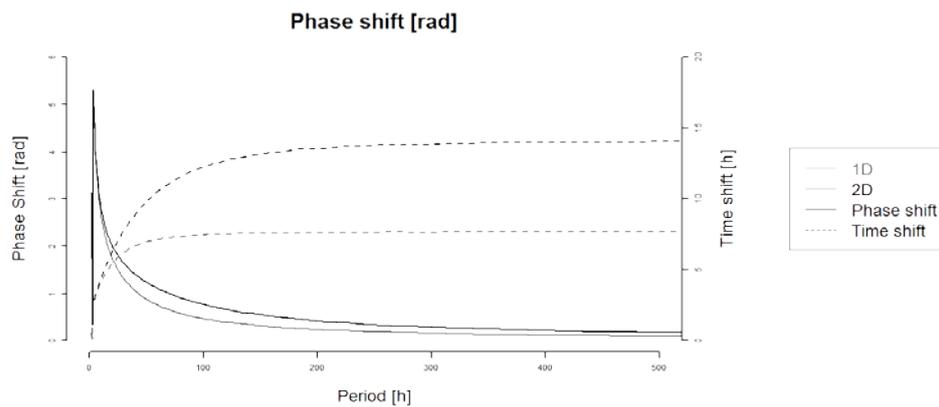

Figure 8: Dynamic thermal transmittance of the architectural junction for the evaluated oscillation periods.

In Figure 9, the dynamic thermal transmittance (Y) value is shown, indicating its evolution towards pseudo-stationary state for long periods. In the one-dimensional model, oscillation periods of 72h or above result in a Y value reaching over 90% of the U-value. In two-dimensional models, 168h are needed to reach such a state.
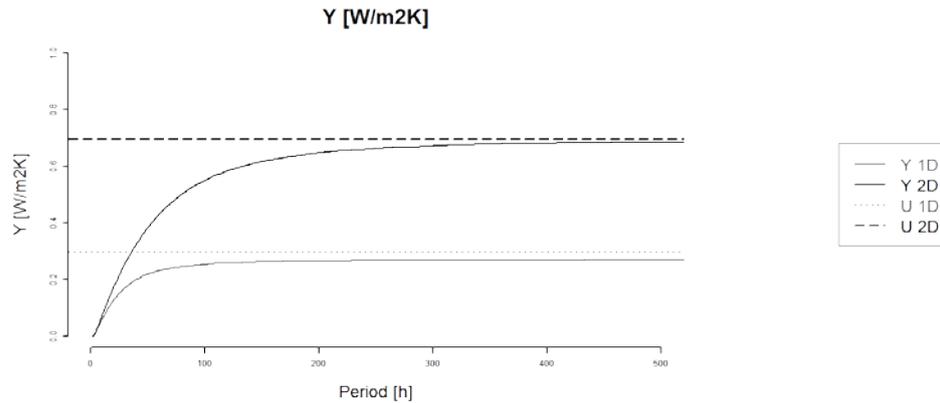
Figure 9: Phase shift of the architectural junction for the evaluated oscillation periods.

The previously mentioned evolution is better assessed with normalized parameters as shown in Figure 10. In this figure, the 1D to 2D normalized difference is shown in terms of periodic thermal transmittance. The difference between both normalized transmittances falls below 10% for oscillation periods greater than 132h.

The relevance of harmonic assessments for very short periods in terms of thermal transmittance can also be assessed. For periods shorter than 6h (1D) and 10h (2D), normalized periodic thermal transmittance is found to be below 10%.
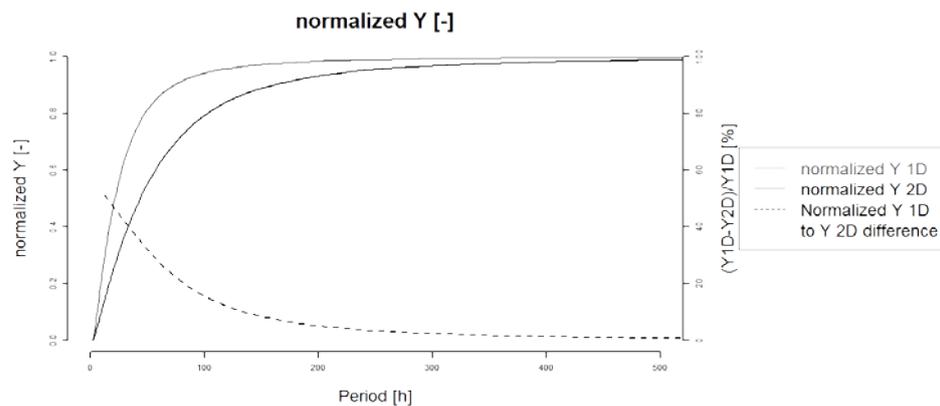

Figure 10: Normalized Y values and differences between 1D and 2D dynamic heat transfer assessments.

Figure 11 presents the harmonic linear thermal coefficient. The magnitude and phase of this phasor are shown. Due to the formulation in (14), the choice of geometrical dimension for the wall height impacts on the resulting parameters. External and internal wall dimensions deviate by 0.3 m over a total floor height of 3.3 m. As such, the harmonic linear thermal coefficient is also different for each considered geometrical criterion. The impact is more clearly seen in terms of magnitude than in terms of phase.
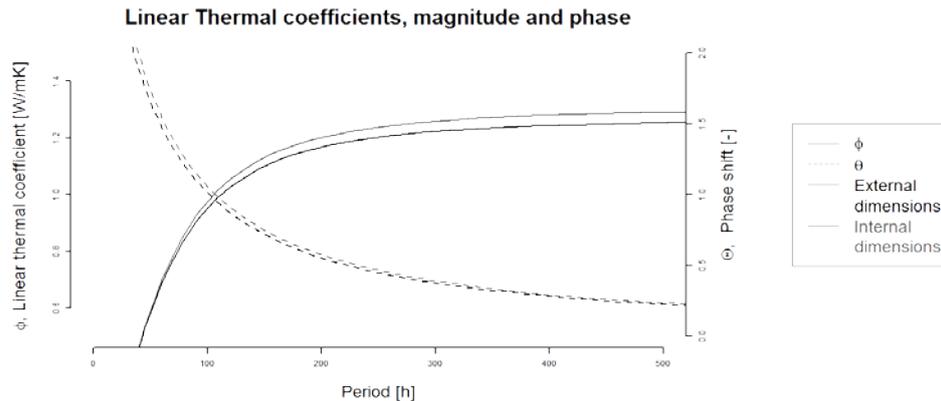
Figure 11: Harmonic linear thermal coefficient, magnitude and phase.

7. Discussion

Based on the outcomes of thermal models developed in this paper, the relevance of a dynamic multi-dimensional thermal assessment of architectural junctions can be assessed.

As it is already known, thermal bridges in architectural junctions are a relevant source of thermal coupling between indoor and outdoor ambiences. This can easily be derived from the steady-state assessment at long periods in Figure 9, where the overall U-value for a 3.3 m high model of an external wall is more than doubled by the architectural junction with an intermediate floor slab. While unsatisfactory, this is an expected behavior for the studied architectural junction. In fact, in many EU national building codes, steady-state thermal bridge calculation is mandatory within the thermal assessment of buildings.

Differences on the dynamic thermal response are observed on the time shift of the architectural junction, which is almost doubled for long oscillation periods.

For long oscillation periods, although the thermal response of 1D and 2D architectural details differs in dynamic thermal transmittance and time shift, the observed differences are relatively stable for oscillation periods greater than 200h. For very rapid oscillations, with periods shorter than 6h, the magnitude of the thermal response is very limited. In this case, although the angular shift may be large, the resulting thermal response is of reduced relevance. However, for intermediate situations, with periods larger than 6h but shorter than 200 h (not reaching quasi-steady-state situations), thermal responses of 1D and 2D cases are relevantly different.

Within the aforementioned range, the dynamic thermal response presents relevant amplitudes, while the dynamics of the heavyweight construction (floor slab) and lightweight construction (insulated façade) clearly differ. In Figure 10, the normalized difference between 1D and 2D cases is not stable and presents large differences, with variations for different oscillation periods. In Figure 8, the variation in phase and time shifts upon oscillation period also shows different behavior for 1D and 2D cases.

For this reason, to the authors' opinion, the dynamic thermal performance of architectural junctions should be considered within the assessment of energy performance of buildings and

their envelopes. This might be of a larger relevance in situations where thermal mass is exposed to both internal and external ambiences, such as the architectural junction in this study, and particularly for climates with highly variable outdoor conditions, in which the predominant heat path is substantially modified. These climatic situations are commonly found in Mediterranean climates in winter periods and in other European climates in summer periods, where indoor temperature is contained within the daily oscillation range of outdoor temperature.

As identified in [23] for steady-state analysis, obtained dynamic thermal bridge parameters differ for each of the geometrical reference systems. As expected, calculations with internal dimensions result in a larger linear thermal bridge coefficient. In the latter case, a smaller one-dimensional heat flow is assumed, which involves a larger correction in the linear thermal bridge coefficient that accounts for the non-one-dimensional heat transfer.

The phasorial analysis proposed in this work serves a dual purpose of analyzing the relevance of the need for dynamic thermal modeling methods for architectural junctions, while developing a suitable mathematical tool for the dynamic modeling of these junctions within a Fourier decomposition of indoor and outdoor boundary conditions.

8. Generalization

In this paper, a generalized formulation is proposed for the assessment of dynamic thermal performance of building envelopes under non-one-dimensional approaches. The presented formulation is valid for 2D and 3D cases, and is built over basic assumptions in the heat transfer analysis of buildings. The generalized formulation follows a similar approach to multidimensional heat transfer in [21], and is based on the linearity of thermal models and the principle of superposition.

Similarly to the approach in [21], all parameters in eq. (12.b, 14 and 16) can be obtained by means of partial models, constructed in such a way that only one particular coefficient is identified in each model according to eq. (16). The proposed formulation is also valid for the calculation of the total harmonic heat transfer of a building envelope, as a dynamic generalization of [35].

The relatively intense computational effort required to obtain the dynamic thermal response of architectural junctions by finite element or finite difference methods implies certain limitations to the present application of this method.

To the authors' belief, this method is not suited for the direct computation of the full procedure for all the excitation periods in each particular case. However, an approach similar to that pursued for simplified calculation of steady-state performance in architectural junctions could be feasible.

Atlases of pre-calculated parameters based on junction topologies are feasible, and phasorial formulations could lead to modified thermal parameters of equivalent walls for later use in prescriptive performance assessments.

For particular cases with heavy thermal integration of one-dimensional and multi-dimensional heat flow, the procedure presented in this work could be pursued for relevant excitation frequencies such as those defined in [32].

9. Mathematical application to BES tools

In this paper, a phasorial formulation is provided for the dynamic computation of multi-dimensional heat transfer in building envelopes. It is considered that this formulation can be developed on a suitable mathematical tool by means of Fourier decomposition of boundary conditions.

However, in the context of BES tools, mathematical approaches such as response factor [43] and z-transfer functions [30, 31] are most commonly used in the computation of heat transfer in building envelopes.

Under this scheme, adaptations are possible where the phasorial approach is replaced by a response factor approach. Following the same process formulated and illustrated in sections 4 and 5 over response factor definitions in [43] an equivalent formulation with a response factor approach can be achieved.

Equation (12.a) can be transformed into (17), where the instantaneous heat transfer is formulated as an aggregation of several 1D, 2D and 3D heat paths.

$$\dot{Q}_{tot} = \sum_{1D} \dot{Q}_i + \sum_{2D} \dot{Q}_j + \sum_{3D} \dot{Q}_k \qquad (17)$$

In (18), heat transfer paths are defined as surface, linear and point heat transfer densities applied over their representative areas and lengths.

$$\dot{Q}_{tot} = \sum_{1D}(\dot{q}_{1D,i} * A_i) + \sum_{2D}(\dot{q}_{2D,j} * l_j) + \sum_{3D}(\dot{q}_{3D,k}) \qquad (18)$$

In (19-22), the dynamic response of the thermal model to its bounding temperatures is formulated. The overall heat transfer across the architectural junction (19), and each of the 1D (20), 2D (21) and 3D (22) heat transfer densities are formulated.

$$\dot{Q}_{tot,t} = \sum_{y=0}^{\infty}(C_{ei,tot,y} * T_{ext,t-y} + C_{ii,tot,y} * T_{int,t-y}) \qquad (19)$$

$$\dot{q}_{1D,i,t} = \sum_{y=0}^{\infty}(c_{ei,1D,i,y} * T_{ext,t-y} + c_{ii,1D,i,y} * T_{int,t-y}) \qquad (20)$$

$$\dot{q}_{2D,j,t} = \sum_{y=0}^{\infty}(c_{ei,2D,j,y} * T_{ext,t-y} + c_{ii,2D,j,y} * T_{int,t-y}) \qquad (21)$$

$$\dot{q}_{3D,k,t} = \sum_{y=0}^{\infty}(c_{ei,3D,k,y} * T_{ext,t-y} + c_{ii,3D,k,y} * T_{int,t-y}) \qquad (22)$$

The relations of dynamic heat flux densities and the dynamic overall heat transfer in the architectural junction in (18) allow formulating (23 and 24) in order to relate response factor in partial formulations (20-22) and overall heat transfer (19).

$$C_{ei,tot,y} = \sum_{1D}(c_{ei,1D,i,y} * A_i) + \sum_{2D}(c_{ei,2D,j,y} * l_j) + \sum_{3D}(c_{ei,3D,k,y}) \qquad (23)$$

$$C_{ii,tot,y} = \sum_{1D}(c_{ii,1D,i,y} * A_i) + \sum_{2D}(c_{ii,2D,j,y} * l_j) + \sum_{3D}(c_{ii,3D,k,y}) \qquad (24)$$

10. Conclusions

Although a dynamic phenomenon, heat transfer in building envelopes has traditionally been addressed by means of steady-state parameters. Dynamic energy assessment of building envelopes is commonly performed by means of numerical simulation in building energy simulation software, where one-dimensional heat transfer is computed. However, there is little background on the dynamic assessment of multi-dimensional heat transfer in architectural junctions. In this paper, a detailed analysis has been performed over a junction of an external wall with an intermediate slab, by means of a phasorial transformation of relevant parameters for the dynamic thermal characteristics of building envelopes in [32], and steady-state parameters in [34] and [21]. The outcomes of this analysis indicate a relevant mismatch between the dynamic thermal response of the one-dimensional wall and the two-dimensional wall-slab junction, in terms of both magnitude and time shift.

The phasorial decomposition proposed in this paper could be taken as a basis to develop a dynamic heat transfer assessment procedure, in which dynamic multi-dimensional heat transfer could be introduced into Building Energy Simulation by means of Fourier decomposition of boundary conditions. However, its present application is limited by the intensive computational time required for obtaining the required dynamic coefficients. Under this approach, the use of junction atlases with pre-calculated data would facilitate the use of this method within BES software.

The proposed approach is valid for mathematical transformations in which linear transformations are possible, such as the Laplace transform, response factor formulation, or Conduction Transfer Function. This roots mathematical applications in the field of heat transfer assessment of building envelopes.

11. Reference

[1] U.S. Department of Energy (DOE), 2008 Buildings Energy Data Book, 2008.

[2] Pérez-Lombard L., et al, A review on buildings energy consumption information, Energy and Buildings 40, 2008

[3] E.U., 2002/91/EC of the European Parliament and of the Council of 16th December 2002 on the Energy Performance of Buildings, 2002.

[4] E.U., 2010/31/EU of the European Parliament and of the Council, of 19 May 2010 on the Energy Performance of Buildings (recast), 2010.

[5] Clarke J.A. Energy simulation in building design. Butterworth-Heinemann, 2nd edition, Oxford (2001).

[6] EnergyPlus v8.4, EnergyPlus™ Documentation, Engineering Reference, https://energyplus.net/sites/default/files/pdfs_v8.3.0/EngineeringReference.pdf (23/02/2016)

[7] TRNSYS 16 Documentation, Volume 6, Multizone Building, http://web.mit.edu/parmstr/Public/Documentation/06-MultizoneBuilding.pdf (23/02/2016)

[8] Strachan, P. ; Monari, F.; Kersken, M. ;Heusler, I. ; IEA Annex 58: Full-scale Empirical Validation of Detailed Thermal Simulation Programs, Energy Procedia 78 (2015), 3288-3293, 6th International Building Physics Conference, IBPC 2015

[9] Zalewski, L., Lassue, S., Rousse, D., & Boukhalfa, K. (2010). Experimental and numerical characterization of thermal bridges in prefabricated building walls. Energy Conversion and Management, 51(12), 2869–2877.

[10] IEE SAVE ASIEPI Project, Assessment and Improvement of the EPBD Impact, "The final recommendations of the ASIEPI project: How to make EPB-regulations more effective? Summary report", 2010, Intelligent Energy Europe programme, contract EIE/07/169/SI2.466278

[11] Schild, P.; Blom, P.: Good practice guidance on thermal bridges and construction details – Part 1: Principles. Information paper 188 (2010). http://www.buildup.eu/publications/8239

[12] Schild, P.: Good practice guidance on thermal bridges and construction details - Part 2: Good examples. Information paper 189 (2010). http://www.buildup.eu/publications/8241

[13] Tilmans, A. (2009). Software and Atlases for evaluating Thermal Bridges. Information paper 152. http://www.buildup.eu/node/5657

[14] IETcc, CEPCO & AICIA, Catálogo De Elementos Constructivos Del Cte, v 6,3, 2010.

[15] Accredited Construction Details (ACDs) for Part L. for England & Wales. 2007, http://www.planningportal.gov.uk/buildingregulations/approveddocuments/partl/bcassociateddocuments9/acd#SteelFrameDetails (2016/02/26)

[16] Enhanced Construction Details (EDCs): Thermal bridging and Airtightness. Energy Saving Trust, UK. http://www.energysavingtrust.org.uk/sites/default/files/reports/CE302%20-%20ECD_thermal%20bridging%20and%20airtightness.pdf (2016/02/26)

[17] Citterio, M. et Al. (2009). Thermal bridges in the EBPD context: overview on MS approaches in regulations. Information paper 64. http://www.buildup.eu/publications/1449

[18] Ge, H., McClung, V. R., & Zhang, S. (2013). Impact of balcony thermal bridges on the overall thermal performance of multi-unit residential buildings: A case study. Energy and Buildings, 60, 163–173.

[19] Karambakkam, B. K., Spitler, J. D., & Leonard, C. M. (2003). A One-dimensional Approximation for Transient Multi- dimensional Conduction Heat Transfer in Building Envelopes, (1995).

[20] Larbi, a. Ben. (2005). Statistical modelling of heat transfer for thermal bridges of buildings. Energy and Buildings, 37(9), 945–951.

[21] EN ISO 10211:2007. Thermal bridges in building construction - Heat flows and surface temperatures - Detailed calculations

[22] T.G. Theodosiou, A.M. Papadopoulos, The impact of thermal bridges on the energy demand of buildings with double brick wall constructions, Energy Build. 40 (11) (2008) 2083–2089.

[23] B. Berggren, M. Wall, Calculation of thermal bridges in (Nordic) building envelopes – risk of performance failure due to inconsistent use of methodology, Energy Build. 65 (2013) 331–339.

[24] DA DB-HE /3, Documento de apoyo al Documento Básico DB-HE Ahorro de la Energía. Puentes Térmicos, Ministerio de Fomento, Spain 2014.

[25] Al-Sanea, S. a. (2003). Finite-volume thermal analysis of building roofs under two-dimensional periodic conditions. Building and Environment, 38(8), 1039–1049.

[26] Martin, K., Erkoreka, a., Flores, I., Odriozola, M., & Sala, J. M. (2011). Problems in the calculation of thermal bridges in dynamic conditions. Energy and Buildings, 43(2-3), 529–535.

[27] Martín, K., Flores, I., Escudero, C., Apaolaza, A., & Sala, J. M. (2010). Methodology for the calculation of response factors through experimental tests and validation with simulation. Energy and Buildings, 42(4), 461–467.

[28] Viot, H., Sempey, a., Pauly, M., & Mora, L. (2015). Comparison of different methods for calculating thermal bridges: Application to wood-frame buildings. Building and Environment, 93, 339–348.

[29] Tadeu, a., Simões, I., Simões, N., & Prata, J. (2011). Simulation of dynamic linear thermal bridges using a boundary element method model in the frequency domain. Energy and Buildings, 43(12), 3685–3695.

[30] Kossecka, E., & Kosny, J. (2004). Two-Step Procedure for Determining Three-Dimensional Conduction Z-Transfer Function Coefficients for Complex Building Envelope Assemblies, ASHRAE, proceeding of Buildings IX: Thermal Performance Of Exterior Envelopes Of Whole Buildings.

[31] Kossecka, E., & Kosny, J. (2005). Three-dimensional conduction z-transfer function coefficients determined from the response factors. Energy and Buildings, 37(4), 301–310.

[32] EN ISO 13786:2007 Thermal performance of building components. Dynamic thermal characteristics. Calculation methods

[33] EN ISO 7345:1996 Thermal Insulation- Physical quantities and definitions

[34] EN ISO 6946:2007 Building components and building elements. Thermal resistance and thermal transmittance. Calculation method

[35] ISO 13789:2007 Thermal performance of buildings -- Transmission and ventilation heat transfer coefficients -- Calculation method

[36] EN 410:2011 Glass in building. Determination of luminous and solar characteristics of glazing

[37] EN 673:2011 Glass in building. Determination of thermal transmittance (U value). Calculation method

[38] Phasor, Wikipedia, https://en.wikipedia.org/wiki/Phasor {2016/03/22}

[39] CEN/TC 89 - Thermal performance of buildings and building components

[40] PHYSIBEL, SOFTWARE for thermal simulation, http://www.physibel.be/ (2017/01/31)

[41] VOLTRA, Computer Program to Calculate 3D & 2D Transient Heat Transfer inObjects Described in a Rectangular Grid Using the Energy Balance Technique,Version 6.3w, Physibel, 2009.

[42] TRISCO, Computer Program to Calculate 3D & 2D Steady State Heat Transfer in Rectangular Objects, Version 12.0w, Physibel, 2010.

[43] Mitalas, G. P.; Stephenson, D. G., Room thermal response factors, ASHRAE Transactions, 73, 1, pp. 1-10, 1967-11-01